Available online at www.sciencedirect.com

ScienceDirect

Ceramics International 40 (2014) 2261–2266

CERAMICS INTERNATIONAL

www.elsevier.com/locate/ceramint

Property optimization of BST-based composite glass ceramics for energy-storage applications

Jinwen Wang, Linjiang Tang, Bo Shen*, Jiwei Zhai

Functional Materials Research Laboratory, Tongji University, Siping Road no. 1239, Shanghai 200092, China

Received 5 July 2013; received in revised form 30 July 2013; accepted 30 July 2013
Available online 8 August 2013

Abstract

A series of $Ba_{0.4}Sr_{0.6}TiO_3$ (BST)-based glass ceramics with different content of BST additive was prepared via sintering and crystallization route, and the subsequent phase evolution, microstructure and dielectric properties were investigated. Results showed that the BST additive obviously improved the dielectric constant of the BST-based glass ceramics. In addition, BST additive can modify the microstructure and reduce the activation energy of grain boundary, which led to an improvement in the dielectric breakdown strengths. The estimated energy density of BST-based glass ceramics with optimized composition reached up to 2.81 J/cm^3, which was improved by 8.5 times as compared with that of the pure glass ceramics (0.33 J/cm^3).

Keywords: D. Glass-ceramics; Barium strontium titanate; Breakdown strength; Activation energy

1. Introduction

Barium strontium titanate (BST) has been highlighted over the past decades as dielectric materials in capacitors, because of their extremely high dielectric constant, low dielectric loss [1,2] and well-controlled Curie temperature by adjusting Ba/Sr ratio [3]. Compared with the conventional ferroelectric ceramics, glass-ceramics with low porosity and high dielectric breakdown strengths (BDS) can provide unique attributes for high-energy density capacitor applications. Up to now, achieving high storage energy density is still a challenging task in glass ceramic systems. The storage energy density for a linear dielectric improves linearly with increasing dielectric constant, whereas it grows quadratically with increasing electric field. So, the high BDS makes a more pronounced contribution towards the energy density. Previous studies [4–9] showed that the BDS was substantially influenced by several factors, such as porosity, grain size, introduction of second phase, temperature, charge injection and interfacial polarization. As was reported [3], the materials with the paraelectric state can maintain good reproductivity at high electric fields. Therefore, $Ba_{0.4}Sr_{0.6}TiO_3$ was selected as the basic composition in this study, whose Curie temperature is about −66 °C.

Several attempts have been made to improve the energy storage density of BST-based glass-ceramics. Divya and Kumar [10] recently reported that partial substitution of SiO_2 by B_2O_3 as a glass former induced uniform distribution of BST ferroelectric crystallites of average size 300 nm in glass matrix. In addition, it has been reported that BaF_2 was helpful in refining the microstructure of BST glass-ceramics and enhancing dielectric constant simultaneously [1]. In our recent work (unpublished), we found that an improved energy storage density can be achieved from BST glass-ceramics annealed by microwave process. However, the enhanced energy storage density in BST glass-ceramics treated by microwave process was mainly derived from the improved dielectric breakdown strengths while less from the dielectric constant. That is, the dielectric constant was still not high enough, although the selected BST-based glass ceramics had a relatively high BDS.

For the application of slurries for tape casting and fabrication of multilayer ceramic capacitors, the BST-based glass ceramic was ground into powders. However, the abnormal growth of particles was observed in the microstructure result.

*Corresponding author. Tel.: +86 21 65980544; fax: +82 21 65985179.
E-mail address: shenbo@tongji.edu.cn (B. Shen).

0272-8842/$ - see front matter © 2013 Elsevier Ltd and Techna Group S.r.l. All rights reserved.
http://dx.doi.org/10.1016/j.ceramint.2013.07.145

In order to increase the dielectric constant and improve the microstructure, the influence of BST powder additive on the dielectric properties of the $BaCO_3$–$SrCO_3$–TiO_2–Al_2O_3–SiO_2 glass-ceramics was studied in the present work. Especially, the effect of BST additive on the microstructure and BDS of BST-based glass ceramics was systematically investigated. Furthermore, the correlation between the dielectric performance and interfacial polarization was also discussed.

2. Experimental procedure

The BST-based glass (BST-G) powders with the composition of $14.8BaCO_3$–$22.2SrCO_3$–$29TiO_2$–$12Al_2O_3$–$22SiO_2$ (mol%) was an aluminum silicate glass from which $Ba_{0.4}Sr_{0.6}TiO_3$ could crystallize at about 916 °C. The powders containing appropriate constituents were ball milled for 20 h in a high-density polyethylene bottle with ethanol as milling media for homogenous mixing. After drying at 120 °C for 6 h, the powders were placed in an alumina crucible and heated to 1550 °C in an elevator furnace for 3.5 h, and then quickly removed from the furnace to be poured into water to get glass powders. Subsequently the glass frit was ball-milled for 20 h to produce powders of fine particle size.

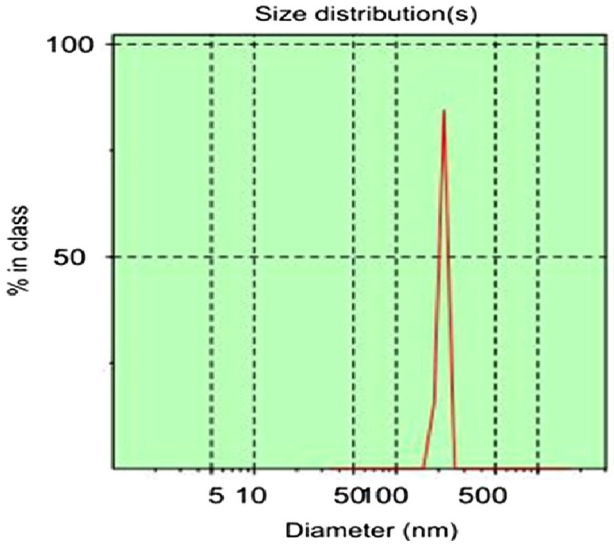

Fig. 1. Size distribution of BST particles distributed in ethanol.

$Ba_{0.4}Sr_{0.6}TiO_3$ (BST) powders were fabricated through chemical solution precipitation [11] with the analytical pure $Ba(OH)_2 \cdot 8H_2O$, $Sr(OH)_2 \cdot 8H_2O$, and $Ti(OBu)_4$. Average particle size of the BST nanopowders was about 200 nm (as shown in Fig. 1).

The two powders were mixed in the ratio according to the following chemical composition: 100 wt% [BST-G] − x wt% BST, where $x=0$ (G-0), $x=50$ (G-50), $x=100$ (G-100), $x=150$ (G-150), and $x=200$ (G-200). The mixed powders were pressed into pellets with 10 mm in diameter and then sintered at 1250 °C for 2 h.

X-ray diffraction (XRD) (D8 Advance, Bruker AXS, Germany) was used to investigate the phase evolution. The polished and thermal-etched surfaces of the sintered samples were examined using field emission scanning electron microscopy (FE-SEM; HITACHI S-4700). The temperature dependences of dielectric constant and dielectric loss were measured using a LCR meter (Agilent E4980A) at the frequency of 1 MHz and in the temperature range from −150 °C to 120 °C. Complex impedance spectrum were carried out by a LCR meter (Agilent E4980A) over frequencies from 150 Hz to 2 MHz in a temperature range of 430–540 °C with an AC electric field of 4 V/mm. The DC dielectric breakdown strength (BDS) measurement was performed using a Voltage-withstand testing device (ET2671B, Entai, Nanjing, China) at room temperature. All samples were ground into about 0.1 mm thickness and immersed in silicone oil to prevent surface flashover.

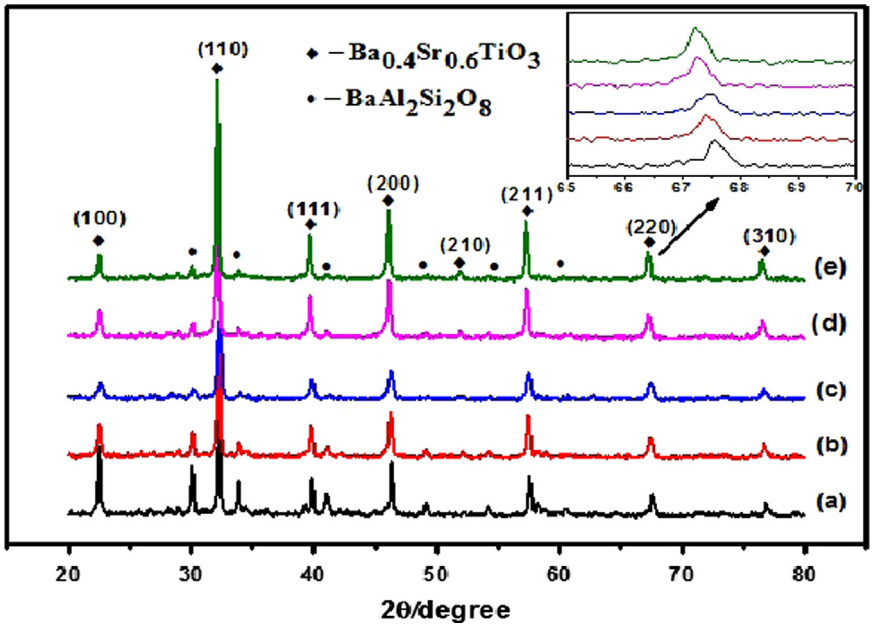

Fig. 2. XRD results of (a) G-0, (b) G-50, (c) G-100, (d) G-150 and (e) G-200.

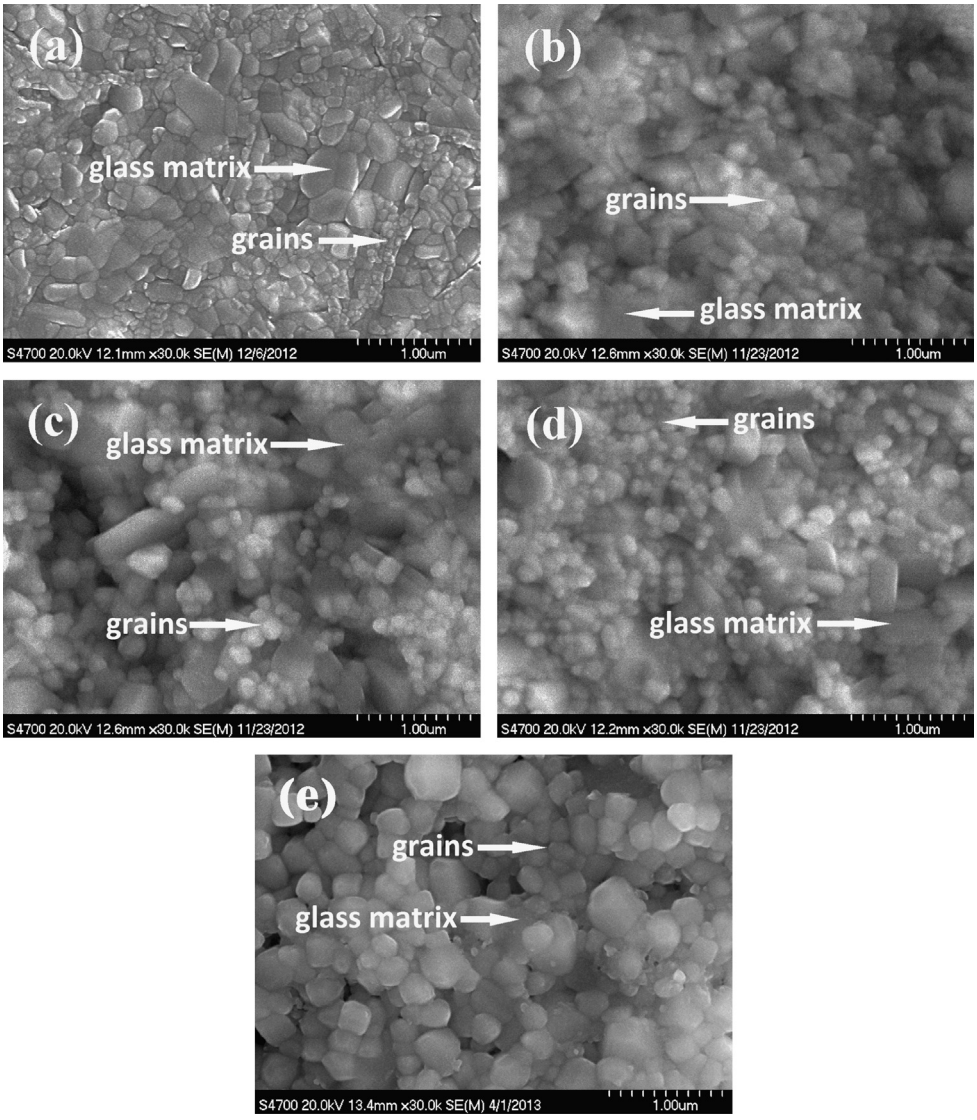

Fig. 3. FE-SEM micrographs of (a) G-0, (b) G-50, (c) G-100, (d) G-150 and (e) G-200.

3. Results and discussion

Fig. 2 shows XRD pattern of the samples. All samples exhibited a perovskite structure with a second phase. The $BaAl_2Si_2O_8$ in the $BaO–TiO_2–SiO_2–Al_2O_3$ system was the only second phase detected by the XRD. Obviously, the relative intensity of the BST peaks obviously increased with increasing the content of BST. Furthermore, the peaks of the BST phase shifted to lower angle with increasing the BST content as illustrated in the inset of Fig. 2, which indicates that the ratio of Ba/Sr increased accordingly.

FE-SEM micrographs of the samples are shown in Fig. 3. For the sample G-0, a large amount of fine grains was crystallized in the glass matrixes, as evident by large particles coexisted with very small grains. Compared with the sample G-0, BST grains dispersed uniformly among the glass matrixes for G-50, G-100, G-150 and G-200 compositions. This preliminary result would cause us to consider that BST additive can cut off the contact among the BST-G powders, which effectively restrain the abnormal growth of the BST-G. In addition, for the G-200 composition, the grain size increased obviously. The result suggests that excess additive of BST will result in increasing the grain size of BST. So, an appropriate amount of BST additive can improve the microstructure homogeneity.

The dielectric–temperature characteristics of the samples containing different amounts of BST over the temperature range of −150 to 120 °C is illustrated in Fig. 4. With the increase of the BST content, the Curie temperature T_c shifted to higher temperature and the dielectric constant increased, which is associated with the increasing ratio of Ba/Sr and BST content in the BST-based glass ceramics. For the BST-G, the Ba/Sr ratio was less than 0.4/0.6 because of the crystallization of $BaAl_2Si_2O_8$. With increasing BST content, Ba/Sr ratio of the composite increased gradually, which is also confirmed by the XRD results (peaks of the BST shifted to lower angle). The variation in dielectric constant (at room temperature) with BST

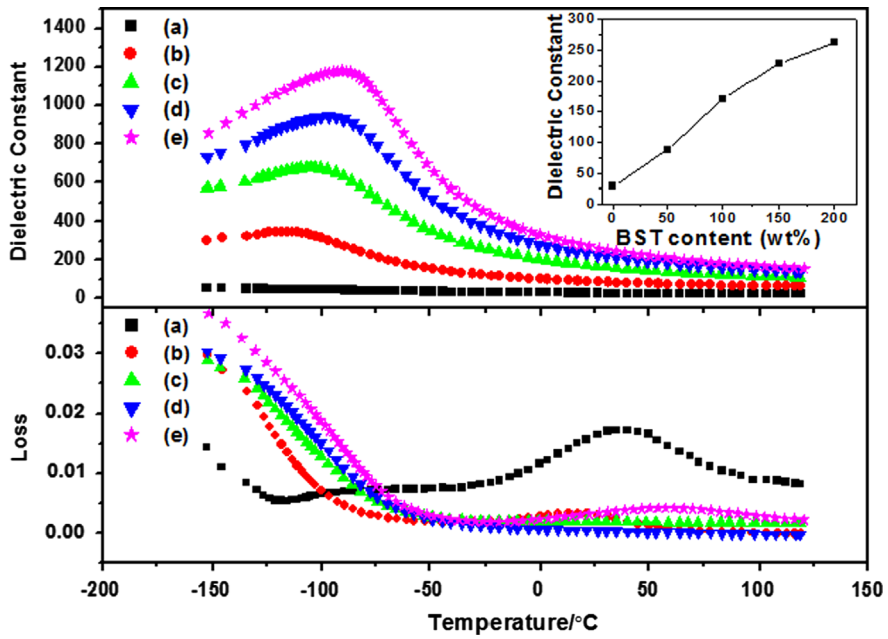

Fig. 4. Temperature dependence of dielectric constant and dielectric loss of (a) G-0, (b) G-50, (c) G-100, (d) G-150 and (e) G-200 (measured at 1 MHz). Inset: dielectric constant at room temperature of the samples.

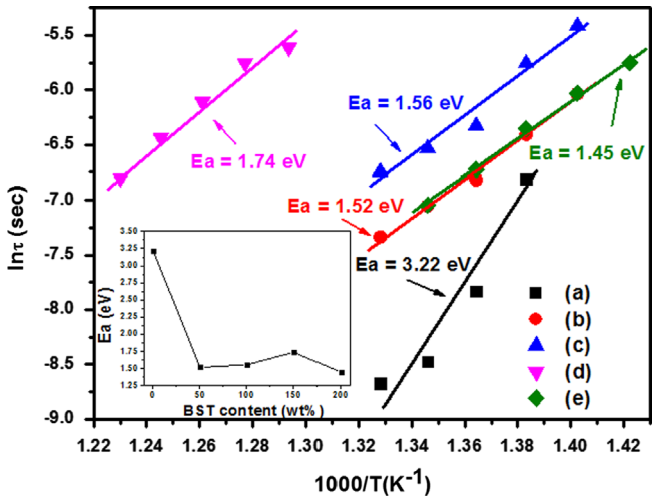

Fig. 5. Relaxation time as a function of 1000/T for (a) G-0, (b) G-50, (c) G-100 and (d) G-150 and (e) G-200 (E_a: the activation energy. The solid lines are linear fits through the data). Inset: E_a of the samples.

content is plotted in the inset of Fig. 4. Plot of the dielectric loss versus temperature for the sample G-0 comprises a maximum value situated at about 50 °C, which is related to interfacial polarization [12]. For the other compositions, the maximum value disappeared and the dielectric loss decreased obviously with the increase of BST content.

The variation of relaxation time as a function of temperature is illustrated in Fig. 5. The relaxation time was obtained from the complex impedance data measured at a certain temperature. And the plots of $\ln \tau$ versus $1/T$ were linear and obeyed the Arrhenius relationship [12], from which the activation energy (E_a) can be obtained. Details of calculation method of the relaxation time (τ) and the activation energy (E_a) can be found elsewhere [9,12]. The E_a characterized the effective traps energy or the interfacial mobility in the defects where polarizability is modified and where charge and energy localization can occur [13]. In this study, the E_a corresponds to the relaxation of space charge at the grain boundary. As was reported [12], an increase in the activation energy of grain boundary suppressed the charge transport across the grain boundary, thereby introducing a higher space charge polarization. Lower value of E_a implied better charge spreading behavior.

The calculated activation energies E_a of the samples can be obtained from the slope of the function between relaxation time and measuring temperature. As seen from the plots of activation energies for the samples with different BST content (inset of Fig. 5), the E_a was significantly decreased when the BST content was increased up to 50 wt% (sample G-50), which is corresponded to better charge spreading behavior. As the BST content increased from 50 wt% to 200 wt%, there was no obvious change in the E_a. The results should be attributed to the similar microstructure homogeneity. For the sample G-0, it may create a high field concentration at the tips as the microstructure of particles or grains size varied significantly, which led to a bad charge spreading behavior. While for the other samples, the electric field concentration can be significantly weakened because of the formation of uniform microstructure. The change of E_a with BST content was a good indication of the decrease of the interfacial polarization, which is confirmed by the dielectric temperature characteristic curves in Fig. 4, showing the depressed dielectric loss [12].

The results of the dielectric breakdown tests on the samples are shown in the Weibull plots [14,15] of Fig. 6, along with the average BDS of the samples containing different BST content (inset of Fig. 6). All the samples exhibited qualitatively similar behavior, and the data fitted linear relation, indicating that the characteristic breakdown strength was adequately described by

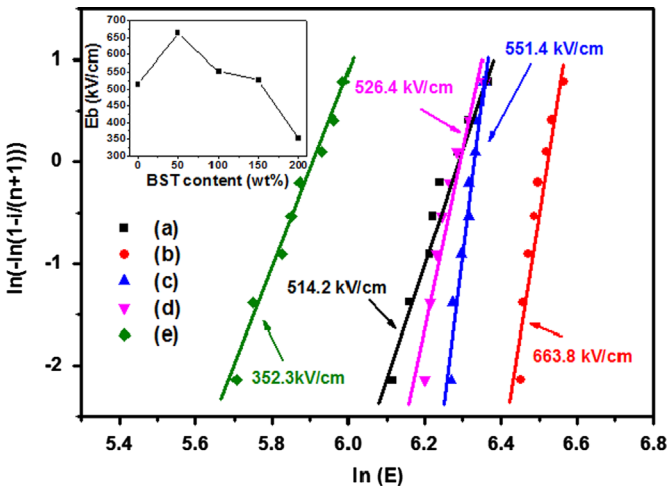

Fig. 6. Weibull plots of dielectric breakdown strength of (a) G-0, (b) G-50, (c) G-100, (d) G-150 and (e) G-200 (E_b: average dielectric breakdown strength). Inset: E_b of the samples.

Table 1
Comparison of relevant dielectric properties and energy densities of the samples.

Samples code	Dielectric constant (room temperature, 1 MHz)	BDS (kV/cm)	Calculated energy density (J/cm^3)
G-0	28.3	514.2	0.33
G-50	87.5	663.8	1.71
G-100	170.1	551.4	2.28
G-150	229.0	526.4	2.81
G-200	263.0	352.3	1.45

Weibull distribution [12]. The BDS increased significantly from 514.2 kV/cm for the sample G-0 to 663.8 kV/cm for the sample G-50. Considering that the dielectric breakdown is related to the charge across the grain boundary space-charge depletion layer in the glass-ceramics [12]. It may cause premature failure at the tips of the inhomogeneous microstructure (sample G-0) where high field concentration can be created, and thus consequently deteriorate the BDS. This improvement in BDS is primarily ascribed to a trade-off between the microstructure homogeneity and the reduction of glass content, wherein homogenous microstructure played a more important role. And the result is in agreement with the charge spreading behavior of interfaces (reflected in Fig. 5) [9,12]. With the further increase of BST content, the BDS decreased to 352.3 kV/cm for the sample G-200, which is attributed to the reduction of glass content. As was reported [12], the BDS can be notably improved with the increase of glass concentration. In this case, the glass concentration decreased with the increase of BST content. Furthermore, the increase of grain size was also deleterious to the BDS [16], which can be reflected in the sample G-200.

The calculated energy densities of the glass-ceramics are summarized in Table 1, which were calculated from the formula $U=0.5\varepsilon_0\varepsilon E^2$. The result indicates that the improved energy density was the combined effect of both the dielectric constant and the BDS. As a consequence, adding a certain amount of BST powders to BST-based glass ceramics had a significant effect on increasing the energy storage density.

4. Conclusions

The microstructure and dielectric properties related with energy storage of the BST-based glass ceramics were investigated as a function of different content of BST additive. It was demonstrated that the additive of BST powders had remarkable influences on the microstructures, dielectric and energy storage properties. The results showed that a certain amount of BST additive can weaken the interfacial polarization by modifying the microstructure homogeneity, which led to a significant improvement in the dielectric breakdown strength. Meanwhile, adding the BST can significantly improve the dielectric constant. The samples with the additive of 50 wt% BST (G-50) had the highest BDS of 663.8 kV/cm, which was 1.3 times higher than that of pure BST-based glass ceramics (G-0). For the sample with the addition of 150 wt% BST (G-150), the storage energy density can be improved up to 2.81 J/cm^3.

Acknowledgments

The authors would like to acknowledge the support from National Key Fundamental Research Program (2009CB623302).

References

[1] E.P. Gorzkowski, M.J. Pan, B. Bender, C.C.M. Wu, Glass-ceramics of barium strontium titanate for high energy density capacitors, Journal of Electroceramics 18 (3–4) (2007) 269–276.
[2] N.H. Fletcher, A.D. Hilton, B.W. Ricketts, Optimization of energy storage density in ceramic capacitors, Journal of Physics D: Applied Physics 29 (1) (1996) 253–258.
[3] E.P. Gorzkowski, M.J. Pan, B.A. Bender, C.C.M. Wu, Effect of additives on the crystallization kinetics of barium strontium titanate glass-ceramics, Journal of the American Ceramic Society 91 (4) (2008) 1065–1069.
[4] Z.H. Wu, H.X. Liu, M.H. Cao, Z.Y. Shen, Z.H. Yao, H. Hao, D.B. Luo, Effect of $BaO–Al_2O_3–B_2O_3–SiO_2$ glass additive on densification and dielectric properties of $Ba_{0.3}Sr_{0.7}TiO_3$ ceramics, Journal of the Ceramic Society of Japan 116 (1350) (2008) 345–349.
[5] T. Tunkasiri, G. Rujijanagul, Dielectric strength of fine grained barium titanate ceramics, Journal of Materials Science Letters 15 (20) (1996) 1767–1769.
[6] A. Young, G. Hilmas, S.C. Zhang, R.W. Schwartz, Effect of liquid-phase sintering on the breakdown strength of barium titanate, Journal of the American Ceramic Society 90 (5) (2007) 1504–1510.
[7] J. Liebault, J. Vallayer, D. Goueriot, D. Treheux, F. Thevenot, How the trapping of charges can explain the dielectric breakdown performance of alumina ceramics, Journal of the European Ceramic Society 21 (3) (2001) 389–397.
[8] M. Touzin, D. Goeuriot, C. Guerret-Piecourt, D. Juve, H.J. Fitting, Alumina based ceramics for high-voltage insulation, Journal of the European Ceramic Society 30 (4) (2010) 805–817.
[9] J.J. Huang, Y. Zhang, T. Ma, H.T. Li, L.W. Zhang, Correlation between dielectric breakdown strength and interface polarization in barium strontium titanate glass ceramics, Applied Physics Letters 96 (4) (2010) 042902.
[10] P.V. Divya, V. Kumar, Crystallization studies and properties of $(Ba_{1-x}Sr_x)TiO3$ in borosilicate glass, Journal of the American Ceramic Society 90 (2) (2007) 472–476.

[11] J.Q. Qi, Y. Wang, W.P. Chen, L.T. Li, H.L.W. Chan, Direct large-scale synthesis of perovskite barium strontium titanate nano-particles from solutions, Journal of Solid State Chemistry 178 (1) (2005) 279–284.
[12] X.R. Wang, Y. Zhang, X.Z. Song, Z.B. Yuan, T. Ma, Q. Zhang, C.S. Deng, T.X. Liang, Glass additive in barium titanate ceramics and its influence on electrical breakdown strength in relation with energy storage properties, Journal of the European Ceramic Society 32 (3) (2012) 559–567.
[13] M. Touzin, D. Goeuriot, H.J. Fitting, C. Guerret-Piecourt, D. Juve, D. Treheux, Relationships between dielectric breakdown resistance and charge transport in alumina materials—effects of the microstructure, Journal of the European Ceramic Society 27 (2–3) (2007) 1193–1197.
[14] J.C. Chen, Y. Zhang, C.S. Deng, X.M. Dai, L.T. Li, Effect of the Ba/Ti ratio on the microstructures and dielectric properties of barium titanate-based glass-ceramics, Journal of the American Ceramic Society 92 (6) (2009) 1350–1353.
[15] A.L. Young, G.E. Hilmas, S.C. Zhang, R.W. Schwartz, Mechanical vs. electrical failure mechanisms in high voltage, high energy density multillayer ceramic capacitors, Journal of Materials Science 42 (14) (2007) 5613–5619.
[16] E.K. Beauchamp, Effect of microstructure on pulse electrical strength of MgO, Journal of the American Ceramic Society 54 (10) (1971) 484–487.